

First-principles Study of Rashba Effect in Ultra-thin Bismuth Surface Alloys

Naoya Yamaguchi^a, Hiroki Kotaka^{a,b}, Fumiyuki Ishii^c

^a*Division of Mathematical and Physical Sciences, Graduate School of Natural Science and Technology, Kanazawa University, Kanazawa 920-1192, Japan.*

^b*Elements Strategy Initiative for Catalysts and Batteries (ESICB), Kyoto University, Kyoto 615-8245, Japan.*

^c*Faculty of Mathematics and Physics, Institute of Science and Engineering, Kanazawa University, Kanazawa 920-1192, Japan.*

Abstract

We performed density functional calculations for ultra-thin bismuth surface alloys: surface alloys of bismuth and face-centered cubic metals Bi/ $M(111)$ - $(\sqrt{3} \times \sqrt{3})R30^\circ$ (M =Cu, Ag, Au, Ni, Co, and Fe). Our calculated Rashba parameters for the Bi/Ag are consistent with the previous experimental and theoretical results. We predicted a trend in the Rashba coefficients α_R of bands around the Fermi energy for noble metals as follows: Bi/Ag > Bi/Cu > Bi/Au. As for the transition metals, there is a trend in α_R : Bi/Ni > Bi/Co > Bi/Fe. Our finding may lead to design efficient spin-charge conversion materials.

Introduction

Strong spin-orbit interaction (SOI) is originated from a heavy element such as bismuth or spatial inversion symmetry breaking, that is, electric field. Rashba-Bychkov effect is induced by SOI [1, 2] and mainly important to spintronics devices such as spin FET (field effect transistor) [3]. The symmetry breaking can take place for the two dimensional electronic gas (2DEG) at the surfaces and interfaces. SOI is attracted attention due to spintronics applications in recent years, and Rashba effect is extensively studied [4].

Spin-to-charge conversion, conversion phenomenon between spin and charge currents, is one of the most important topics in spintronics. Spin current is generated by spin Seebeck effect (SSE) [5], for example. SSE can transform temperature gradient into spin current besides charge current which originate from normal Seebeck effect. Spin-to-charge conversion is important to convert spin current into charge current so effectively as to increase thermoelectric conversion efficiency using the spin Seebeck effect. Inverse spin hall effect (ISHE) is known as such a conversion mechanism [6]. Recently, for a Bi/Ag Rashba interface, a large conversion phenomenon between spin and charge currents has been reported [7]. That spin-to-charge conversion is induced by the inverse Rashba-Edelstein effect (IREE) on the metal-metal or metal-insulator interface with strong SOI, which is the inverse process of Edelstein effect [8]. The strength of the IREE is related with the Rashba coefficient α_R , which reflects the strength of the Rashba effect. IREE can be used for an alternative mechanism of detection of spin current utilizing ISHE. Indeed, giant

Rashba spin splitting in Bi/Ag surface alloys was reported [9, 10].

In this paper, we investigated the Rashba effects for surface alloys composed of Bi and 3d-transition metals (Fe, Co, Ni) and noble metals (Cu, Ag, Au) using first-principles calculations. The trend in the surface alloys can be considered to be similar with that in the corresponding interfaces. One of our results for noble metals is that there is a trend in the order of magnitude of α_R for bands around Fermi energy: Bi/Ag > Bi/Cu > Bi/Au.

Methods

For the two dimensional electronic system perpendicular to the direction of electric field, the Hamiltonian to be considered is the sum of the kinetic energy of free electron gas and Rashba Hamiltonian which can be expressed by

$$H_R = \alpha_R(\hat{e}_z \times \vec{k}_{||}) \cdot \vec{\sigma} = \alpha_R(k_y\sigma_x - k_x\sigma_y),$$

where α_R denotes the Rashba coefficient, \hat{e}_z the unit vector along z axis, $\vec{k}_{||} = (k_x, k_y, 0)$ the wave vector, and $\vec{\sigma} = (\sigma_x, \sigma_y, \sigma_z)$ the Pauli matrices vector. We can solve the eigen value problem for that Hamiltonian, and obtain the energy dispersion relation for the nearly free electron under the Rashba effect:

$$E_{\pm}(\vec{k}_{||}) = \frac{\hbar^2 k_{||}^2}{2m^*} \pm \alpha_R k_{||},$$

where \hbar is the Planck constant, and m^* the effective mass of electrons. Then, the Rashba coefficient can be obtained as follows: $\alpha_R = 2E_R/k_R$ where $E_R = m^* \alpha_R^2 / (2\hbar^2)$ is the Rashba energy, and $k_R = m^* \alpha_R / \hbar^2$ the Rashba momentum offset.

We performed density functional calculations within the local spin density approximation [11] using OpenMX code

Email addresses: n-yamaguchi@cphys.s.kanazawa-u.ac.jp (Naoya Yamaguchi), ishii@cphys.s.kanazawa-u.ac.jp (Fumiyuki Ishii)

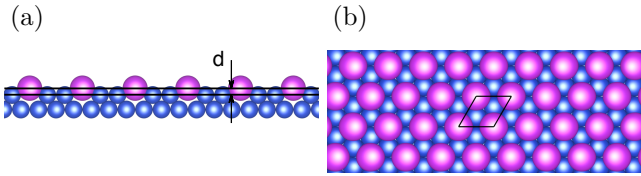


Figure 1: Atomic structure of the Bi/ M surface alloy. (a) Side view. d denotes the corrugation parameter. (b) Top view. the rhombus represents the unit cell. The in-plane cell length is $(\sqrt{6}/2)a_M$, where a_M is the lattice constant for $M(100)$.

[12], with the fully relativistic total angular momentum dependent pseudopotentials taking SOI into account [13]. We adopted norm-conserving pseudopotentials with an energy cutoff of 200 Ry for charge density including $5d$, $6s$, and $6p$ -states as valence states for Bi; the $3s$, $3p$, $3d$, and $4s$ for Cu, Ni, Co, and Fe; $4p$, $4d$, and $5s$ for Ag; $5p$, $5d$, and $6s$ for Au. We used $8 \times 8 \times 1$ k-point mesh. In this calculation, the numerical pseudo atomic orbitals are utilized as follows: For all models, the numbers of the s -, p -, and d -character orbitals are three, three, and two, respectively; The cutoff radiuses of Bi, Cu, Ag, Au, Ni, Co, and Fe are 8.0, 6.0, 7.0, 7.0, 6.0, 6.0, and 6.0, respectively, in units of Bohr. The dipole-dipole interaction between slab models can be eliminated by the effective screening medium (ESM) method [14].

Models

Bismuth surface alloys are thermodynamically stable and can be synthesized on noble metal surfaces [15]. Figure 1 shows the computational model of a surface alloy composed of the bismuth and face-centered cubic metal. We assumed here the freestanding Bi/ M (M =Cu, Ag, Au, Fe, Co, and Ni) surface alloy model to be the structure where $1/3$ M atoms on the topmost atomic layer are replaced with Bi atoms. The structure is based on Bi/Ag and Bi/Cu(111)- $(\sqrt{3} \times \sqrt{3})R30^\circ$ surface alloys of the prior studies [9, 16]. We defined the length between the Bi and M atoms as the corrugation parameter d (See Fig. 1(a)). We adopted the 2-atomic-layer model (e.g. a Bi/Ag surface alloy its underlying Ag atomic layer) for optimizing d , and 1-atomic-layer model (e.g. only the Bi/Ag alloy) for calculating the band structure of each freestanding surface alloy, respectively. The 2-atomic-layer model was used for the computational model in the previous study [10]. We used the experimental lattice constants for each surface alloy model shown in Tab. 1. Our calculated values of d for the Bi/Ag and Bi/Cu surface alloys are consistent with the experimental ones [9, 16].

Results and Discussion

Figure 2(a)-(c) shows the band structures for the freestanding surface alloys composed of bismuth and noble metals (Cu, Ag, Au). There are two notable Rashba splittings of free-electron-like bands around Γ -point for each surface alloy. The Rashba bands are $3/4$ filled with valence electrons. We focused on the both splittings in the band structures, and evaluated the Rashba parameters: k_R , E_R , and α_R (See Tab. 2).

In the case of the Bi/Ag surface alloy, our calculated values for the lower Rashba splitting in the Bi/Ag surface alloy ($k_R=0.124 \text{ \AA}^{-1}$; $E_R=0.177 \text{ eV}$; $\alpha_R=2.85 \text{ eV}\cdot\text{\AA}$) are agreement with experimental ones ($k_R=0.13 \text{ \AA}^{-1}$; $E_R=0.2 \text{ eV}$; $\alpha_R=3.05 \text{ eV}\cdot\text{\AA}$ [9]). Besides, Our result that the Rashba momentum offset k_R is the value of 0.124 \AA^{-1} for the lower splitting, and 0.075 \AA^{-1} for the upper, respectively, are also consistent with those of the previous theoretical study [10]: $k_R=0.144 \text{ \AA}^{-1}$ at $d=0.65 \text{ \AA}$ for the lower, and $k_R=0.09 \text{ \AA}^{-1}$ at $d=0.8 \text{ \AA}$ for the upper.

For the Bi/Cu alloy, the Rashba coefficient α_R of the Bi/Cu is comparable to that of the Bi/Ag. However, our results for the Bi/Cu differ from the earlier studies, where the Rashba parameters of $k_R=0.03 \text{ \AA}^{-1}$, $E_R=0.015 \text{ eV}$, and $\alpha_R=1 \text{ eV}\cdot\text{\AA}$ were reported [15]. That difference might be caused by the thickness of Cu in the computational model, for our calculated values for the 10-atomic-layer model are $k_R=0.036 \text{ \AA}^{-1}$, $E_R=0.015 \text{ eV}$, and $\alpha_R=0.83 \text{ eV}\cdot\text{\AA}$. For the Bi/Au alloy, the Rashba coefficient α_R is slightly smaller compared with the other noble metal alloys. There is a trend in the order of magnitude of α_R : Bi/Ag > Bi/Cu > Bi/Au (the lower splitting); Bi/Cu > Bi/Ag > Bi/Au (the upper splitting). Since the lower splitting is larger than the upper one in the momentum offset k_R , the lower is seemed to be more important to transport properties if the Fermi level lies around it.

We also calculated the Bi/Ni, Bi/Co, and Bi/Fe surface alloys under non-magnetic condition. Figure 3(a)-(c) shows the band structures for the freestanding surface alloys composed of bismuth and $3d$ -transition metals (Ni, Co, Fe). As with the surface alloys composed of Bi and noble metals, there are two Rashba splittings for each surface alloys. As for the transition metals, there is a trend in Rashba parameters for both splittings: Bi/Ni > Bi/Co > Bi/Fe (See Tab. 2).

The Rashba coefficient α_R are thought to originate from the asymmetry of the surface state (SS) [23, 24]. The mechanism of the Rashba-Bychkov effect at the surface due to the asymmetric SS was explained using an expression: $\alpha_R = (2/c^2) \int d\vec{r} \partial_z V |\psi_{SS}|^2$, where c is the speed of light, V the potential, and ψ_{SS} the wave function of SS [23]. As mentioned above, in the case of the Bi/Cu alloy, our calculated α_R for 1- and 10-atomic-layer model are 2.59 and $0.83 \text{ eV}\cdot\text{\AA}$, respectively, and thus, the magnitude of α_R is strongly dependent on the thickness of Cu. However, for the Bi/Ag alloy, α_R is insensitive to the thickness of Ag ($2.85 \text{ eV}\cdot\text{\AA}$ (1-atomic-layer); $2.82 \text{ eV}\cdot\text{\AA}$ (10-atomic-layer)).

Table 1: Lattice constants a_M for $M(100)$ and optimum corrugation parameters d for each surface alloy model Bi/ M .

Bi/ M	Bi/Cu	Bi/Ag	Bi/Au	Bi/Ni	Bi/Co	Bi/Fe
$a_M(\text{\AA}, \text{expt.})$	3.615[17]	4.1[17]	4.0773[18]	3.53[19]	3.5656[20]	3.613[21]
$d(\text{\AA})$	1.015	0.690	0.785	0.912	0.929	1.043
$d(\text{\AA}, \text{expt.})$	1.02[16]	0.65[22]	-	-	-	-

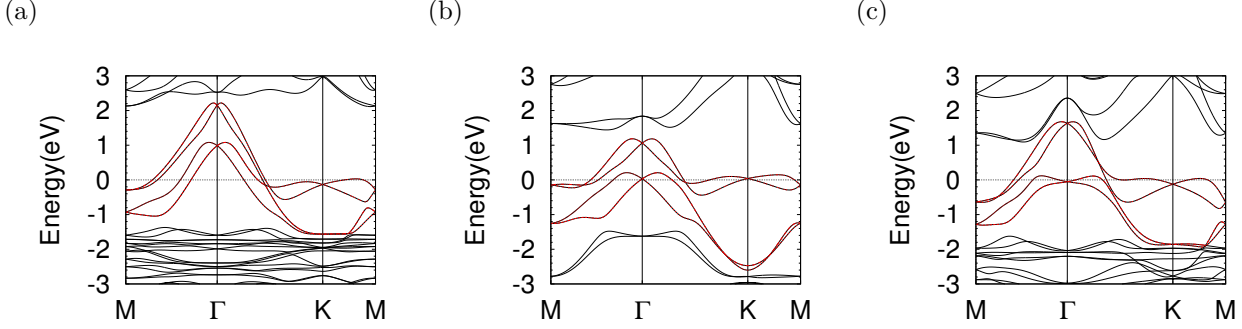


Figure 2: Band structures for each freestanding surface alloy: (a) Bi/Cu; (b) Bi/Ag; (c) Bi/Au.

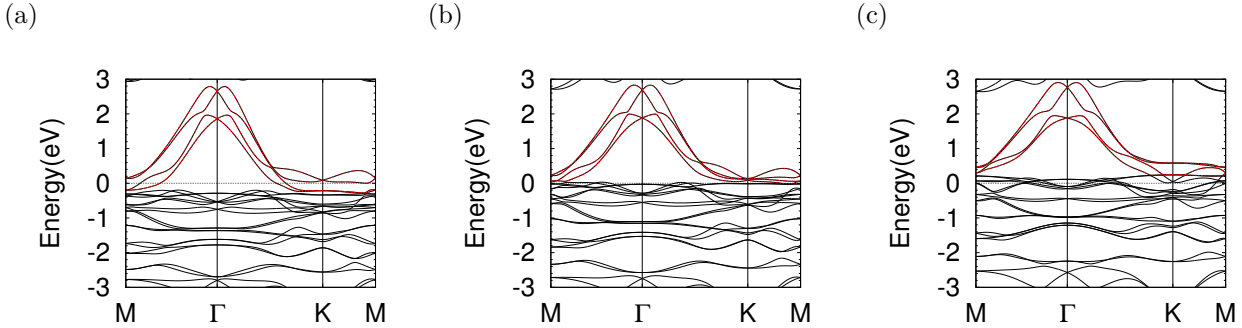


Figure 3: Band structures for each freestanding surface alloy: (a) Bi/Ni; (b) Bi/Co; (c) Bi/Fe.

Table 2: Rashba parameters in the Bi/ M alloys: α_R is the Rashba coefficient, E_R the Rashba energy, k_R the Rashba momentum offset.

M	Cu	Ag	Au	Ni	Co	Fe
(Upper splitting)						
$k_R(\text{\AA}^{-1})$	0.036	0.075	0.046	0.067	0.077	0.082
$E_R(\text{eV})$	0.068	0.123	0.044	0.135	0.140	0.139
$\alpha_R(\text{eV}\cdot\text{\AA})$	3.76	3.28	1.91	4.05	3.71	3.40
(Lower splitting)						
$k_R(\text{\AA}^{-1})$	0.072	0.124	0.206	0.094	0.113	0.115
$E_R(\text{eV})$	0.093	0.177	0.168	0.107	0.112	0.067
$\alpha_R(\text{eV}\cdot\text{\AA})$	2.59	2.85	1.63	2.28	1.98	1.17

This difference between the Bi/Cu and Bi/Ag may be due to the difference in the degree of the localization of SS, and in terms of the thickness dependence of M , its localization is seemed to be stronger for the Bi/Ag than Bi/Cu. Indeed, it was reported that the strong localized SS exists for the Bi/Ag alloy [10, 15]. For all the 1-atomic-layer model, α_R is so large as to comparable with the Bi/Ag surface alloy, with the thinness of the surface alloy films confining the wave functions including the SS. In other words, the strong localization of the SS may enhance the asymmetry of the charge distribution for the SS, which makes α_R large. The localization of the SS as well as the corrugation parameter d may be important to α_R .

Conclusion

We performed density functional calculations for ultra-thin bismuth surface alloys: Bi/ $M(111)$ - $(\sqrt{3} \times \sqrt{3})R30^\circ$, and calculated Rashba parameters to predict its trend for two notable Rashba splittings of free-electron-like bands around Γ -point. For noble metals, we found a trend in the Rashba coefficients α_R : Bi/Ag > Bi/Cu > Bi/Au (the lower splitting); Bi/Cu > Bi/Ag > Bi/Au (the upper splitting). The lower values may be important to transport properties because the lower is larger in the momentum offset k_R . As for the transition metals, there is a trend in α_R : Bi/Ni > Bi/Co > Bi/Fe. Not only the corrugation parameter d but the localization of the surface states may be important to α_R . Our finding may lead to design efficient spin-charge conversion materials.

Acknowledgements

The authors thank K. Kondou for invaluable discussions. This work was supported by Grant-in-Aid for Scientific Research on Innovative Area, "Nano Spin Conversion Science" (Grant No.15H01015). The work was partially supported by Grants-in-Aid on Scientific Research under Grant Nos. 25790007 and 16K04875 from Japan Society for the Promotion of Science. This work was also supported in part by MEXT as a social and scientific priority issue (Creation of new functional devices and high-performance materials to support next-generation industries) to be tackled by using post-K computer. Computations in this research were also performed using supercomputers at ISSP.

References

[1] Y. A. Bychkov, E. I. Rashba, JETP Lett. 39 (1984) 78–81.
 [2] S. LaShell, B. McDougall, E. Jensen, Phys. Rev. Lett. 77 (1996) 3419–3422.
 [3] S. Datta, B. Das, Appl. Phys. Lett. 56 (1990) 665.
 [4] K. Ishizaka, M. Bahramy, H. Murakawa, M. Sakano, T. Shimajima, T. Sonobe, K. Koizumi, S. Shin, H. Miyahara, A. Kimura, K. Miyamoto, T. Okuda, H. Namatame, M. Taniguchi, R. Arita, N. Nagaosa, K. Kobayashi, Y. Murakami, R. Kumai, Y. Kaneko, Y. Onose, Y. Tokura, Nat. Mater. 10 (2011) 521–526.
 [5] K. Uchida, S. Takahashi, K. Harii, J. Ieda, W. Koshibae, K. Ando, S. Maekawa, E. Saitoh, Nature 455 (2008) 778–781.

[6] E. Saitoh, M. Ueda, H. Miyajima, G. Tatara, Appl. Phys. Lett. 88 (2006) 182509.
 [7] J. C. R. Sánchez, L. Vila, G. Desfonds, S. Gambarelli, J. P. Attané, J. M. D. Teresa, C. Magén, A. Fert, Nat. Commun. 4 (2013) 2944.
 [8] V. M. Edelstein, Solid State Commun. 73 (1990) 233–235.
 [9] C. Ast, J. Henk, A. Ernst, L. Moreschini, M. Falub, D. Pacilé, P. Bruno, K. Kern, M. Grioni, Phys. Rev. Lett. 98 (2007) 186807.
 [10] G. Bian, X. Wang, T. Miller, T. Chiang, Phys. Rev. B 88 (2013) 085427.
 [11] D. Ceperley, B. Alder, Phys. Rev. Lett. 45 (1980) 566–569.
 [12] T. Ozaki, H. Kino, J. Yu, M. Han, M. Ohfuchi, F. Ishii, OpenMX, <http://www.openmx-square.org/>.
 [13] G. Theurich, N. A. Hill, Phys. Rev. B 64 (2001) 073106.
 [14] M. Otani, O. Sugino, Phys. Rev. B 73 (2006) 115407.
 [15] L. Moreschini, A. Bendounan, H. Bentmann, M. Assig, K. Kern, F. Reinert, J. Henk, C. Ast, M. Grioni, Phys. Rev. B 80 (2009) 035438.
 [16] D. Kaminski, P. Poodt, E. Aret, N. Radenovic, E. Vlieg, Surf. Sci. 575 (2005) 233–246.
 [17] R. Ingen, R. Fastenau, E. Mittemeijer, J. Appl. Phys. 76 (1994) 1871.
 [18] M. Ellner, K. Kolatschek, B. Predel, J. Less-Common Met. 170 (1991) 171–184.
 [19] J. W. Cable, Y. Tsunoda, J. Magn. Magn. Mater. 140 (1995) 93–94.
 [20] M. Singh, M. Barkei, G. Inden, S. Bhan, Phys. Status Solidi A 87 (1985) 165–168.
 [21] W. F. Schlosser, Phys. Status Solidi A 17 (1973) 199–205.
 [22] I. Gierz, B. Stadtmüller, J. Vuorinen, M. Lindroos, F. Meier, J. Dil, K. Kern, C. Ast, Phys. Rev. B 81 (2010) 245430.
 [23] M. Nagano, A. Kodama, T. Shishidou, T. Oguchi, J. Phys. Condens. Matter 21 (2009) 064239.
 [24] H. Bentmann, T. Kuzumaki, G. Bihlmayer, S. Blügel, E. Chulkov, F. Reinert, K. Sakamoto, Phys Rev B 84 (2011) 115426.